

# Linköping University Post Print

## Competition between Magnetic Structures in the Fe-Rich FCC FeNi Alloys

Igor A. Abrikosov, Andreas E. Kissavos, Francois Liot, Björn Alling, Sergey Simak,  
O. Peil and A. V. Ruban

N.B.: When citing this work, cite the original article.

Original Publication:

Igor A. Abrikosov, Andreas E. Kissavos, Francois Liot, Björn Alling, Sergey Simak, O. Peil and A. V. Ruban, Competition between Magnetic Structures in the Fe-Rich FCC FeNi Alloys, 2007, Physical Review B Condensed Matter, (76), 1, 014434.

<http://dx.doi.org/10.1103/PhysRevB.76.014434>

Copyright: American Physical Society

<http://www.aps.org/>

Postprint available at: Linköping University Electronic Press

<http://urn.kb.se/resolve?urn=urn:nbn:se:liu:diva-14277>

## Competition between magnetic structures in the Fe rich fcc FeNi alloys

I. A. Abrikosov,<sup>1</sup> A. E. Kissavos,<sup>1</sup> F. Liot,<sup>1</sup> B. Alling,<sup>1</sup> S. I. Simak,<sup>1</sup> O. Peil,<sup>2</sup> and A. V. Ruban<sup>2</sup>  
<sup>1</sup>*Department of Physics, Chemistry and Biology (IFM), Linköping University, SE-581 83 Linköping, Sweden*  
<sup>2</sup>*Applied Materials Physics, Department of Materials Science and Engineering, Royal Institute of Technology, SE-10044 Stockholm, Sweden*

(Received 21 March 2007; published 27 July 2007)

We report on the results of a systematic *ab initio* study of the magnetic structure of Fe rich fcc FeNi binary alloys for Ni concentrations up to 50 at. %. Calculations are carried out within density-functional theory using two complementary techniques, one based on the exact muffin-tin orbital theory within the coherent potential approximation and another one based on the projector augmented-wave method. We observe that the evolution of the magnetic structure of the alloy with increasing Ni concentration is determined by a competition between a large number of magnetic states, collinear as well as noncollinear, all close in energy. We emphasize a series of transitions between these magnetic structures, in particular we have investigated a competition between disordered local moment configurations, spin spiral states, the double layer antiferromagnetic state, and the ferromagnetic phase, as well as the ferrimagnetic phase with a single spin flipped with respect to all others. We show that the latter should be particularly important for the understanding of the magnetic structure of the Invar alloys.

DOI: 10.1103/PhysRevB.76.014434

PACS number(s): 75.30.-m, 75.50.Bb

### I. INTRODUCTION

Investigations of the magnetic properties of Fe-based alloys are important from the fundamental as well as applied points of view. Indeed, Fe is among the most abundant elements on Earth, and is probably the major alloy component for the modern industry. Its structural and magnetic phase diagrams are enormously rich. At ambient conditions, it is stable in the body centered cubic phase (bcc), which is ferromagnetic. With increasing temperature it first becomes paramagnetic above the Curie temperature of 1043 K, and then transforms structurally into the face centered cubic (fcc) phase at 1183 K. Just before melting, Fe re-enters the paramagnetic bcc phase. At relatively low temperatures, it transforms into the hexagonal closed-packed structure (hcp) at pressure above 13 GPa.<sup>1</sup> A competition between antiferromagnetism and superconductivity was reported for iron at these conditions.<sup>2</sup>

The situation becomes even more complicated and intriguing with alloying. Different elements may stabilize either the bcc or fcc phases in the alloy at ambient pressure, and could strongly affect the magnetic and mechanical properties of Fe. Moreover, it has become absolutely clear that magnetism in Fe-based alloys has a very strong influence on the thermodynamic properties, phase stabilities, and elastic properties of these materials. One of the most remarkable examples here is the Invar effect observed in FeNi alloys by Guillaume more than 100 years ago,<sup>3</sup> which consists of the vanishing of the thermal expansion coefficient of the fcc FeNi steels at Ni concentrations around 35 at. %. This effect has attracted a lot of attention, and an excellent review of the early work can be found in, e.g., Ref. 4. Moreover, in recent years theoretical as well as experimental communities have demonstrated an increased interest in the problem,<sup>5-15</sup> because of new suggestions on the origin of the Invar effect in the FeNi system related to an observation of noncollinear magnetic structures in the alloy.<sup>16</sup>

As a matter of fact, studies of the noncollinear magnetism of pure fcc Fe represent a research field on their own. Experimentally, fcc Fe is stabilized as precipitates in fcc Cu bulk. The precipitates show a lattice constant only 0.7% smaller than the Cu lattice constant for precipitate radii less than 40 nm.<sup>17</sup> For larger precipitates, a structural phase transition to a periodic shear wave occurs.<sup>18</sup> The phase transition can be suppressed by introducing a small amount of Co (4%), which allows for precipitates with as large radii as 100 nm.<sup>17</sup> For the cubic Fe precipitates, the ground state is found to be a spin spiral, with a  $\mathbf{q}$  vector  $\mathbf{q}=[0, \xi_{XW}, 1]$ , where  $\xi_{XW}=0.127$ ,<sup>17</sup> on the path between the special points X and W in the fcc Brillouin zone.

Many theoretical studies devoted to first-principles investigations of the complex magnetic structures of the fcc Fe have been carried out recently.<sup>19-23</sup> A rather complete summary of the theoretical work can be found in Ref. 22, where probably the most accurate calculations are presented. Indeed, the authors considered the full one-electron potential, included the effects of gradient corrections to the potential, and also considered the magnetization density without any restriction to the intra-atomic collinearity. The authors found that the most stable magnetic structure of Fe depended sensitively on volume. At the experimental volume  $a=3.61$  Å, the moments were ordered in collinear double-layer antiferromagnetic structure, while the ground state was almost degenerate between two different helices at equilibrium volumes  $a=3.507$  Å and  $a=3.497$  Å, respectively. Similar conclusions were obtained in highly accurate calculations by Knöpfle *et al.*,<sup>21</sup> where the experimental spin spiral state was also stabilized, but again at somewhat smaller volumes as compared to the experiment. In summary, though the theoretical studies on pure fcc Fe do not exactly reproduce the experimental results on the Fe precipitates in Cu, there is a consensus in the field on the existence and importance of noncollinear magnetism in this material.

The situation is somewhat different in the case of alloys. Magnetic properties of the FeNi system in the whole range

of compositions were studied by several groups.<sup>5,20,24–28</sup> All these studies assumed collinear (ferromagnetic or disordered local moment) structures of the alloy. On the other hand, based on results of a first principles simulation carried out for a large supercell, Wang *et al.*<sup>29</sup> reported an observation of a noncollinear magnetic configuration in an FeNi alloy with a Ni composition of 35 at. % at the theoretical lattice parameter. van Schilfhaarde *et al.*<sup>16</sup> discovered a continuous transition from the ferromagnetic high-spin state at large volumes to increasingly noncollinear disordered magnetic structures at smaller volumes in the Fe<sub>64</sub>Ni<sub>36</sub> fcc alloy in calculations using a 32-atom supercell and the linear muffin-tin orbital (LMTO) method. Olovsson and Abrikosov<sup>30</sup> investigated the dependence of the exchange interactions across the 3*d* transition metal series, and arrived at the conclusion that there exists a region of volumes and electron concentrations with anomalous behavior of the exchange parameters, which could lead to complex magnetic structures. From considerations based on an analysis in the reciprocal space, a similar conclusion was obtained by Lizzáraga *et al.*<sup>6</sup> In Refs. 7 and 31 an importance of the local chemical environment for the magnetic phase transition around the Invar composition was emphasized. Still, despite the importance of these problem, e.g., for the experimental community, and the existence of controversial experimental reports on the observation of the noncollinear magnetism in Invar systems,<sup>12–15</sup> no systematic study of the complex magnetic structures was carried out for the FeNi alloys. Moreover, while for pure Fe the majority of recent calculations employ the generalized gradient approximation<sup>32,33</sup> for the exchange-correlation energy and one-electron potential,<sup>21–23</sup> studies on the alloys<sup>5,20,24–28</sup> are mostly done within the local spin density approximation (LSDA).<sup>34–36</sup> Thus it is important to investigate the effect of gradient corrections on the magnetic structure of the FeNi alloys.

In this work, we study the magnetic structure of the Fe rich fcc FeNi binary alloys for Ni concentrations up to 50 at. % using two complementary techniques, the exact muffin-tin orbital theory within the coherent potential approximation<sup>37</sup> and the projector augmented-wave method<sup>38</sup> as implemented in the Vienna *Ab Initio* Simulation Package.<sup>39,40</sup> We are especially interested in a series of transitions between several competing magnetic structures, including the ferromagnetic phase, the configurations with complete or partial disorder of local magnetic moments, spin spiral states, the single and the double layer antiferromagnetic state, and the ferrimagnetic phase with a single spin flipped with respect to all other spins. The paper is organized as follows: We first describe our methodology. From a consideration of the results obtained for pure fcc Fe, we analyze approximations used in our treatment of the FeNi alloys. The evolution of the alloy magnetic structure with increasing Ni concentration obtained in our EMTO-CPA calculations is presented in Sec. IV. In Sec. V we go beyond the mean-field treatment of the disorder effects, and present results obtained from supercell simulations at the Invar composition. In Sec. VI we discuss and in Sec. VII we summarize the results of this study.

## II. COMPUTATIONAL METHODOLOGY

### A. Treatment of the substitutional disorder

We have simulated substitutional disorder in the FeNi system using two complimentary approaches, the coherent potential approximation (CPA)<sup>41</sup> and the supercell approach. The former approximation, originally introduced by Soven<sup>42</sup> for the electronic structure problem and by Taylor<sup>43</sup> for phonons in random alloys, is currently one of the most popular techniques to deal with substitutional disorder. In the CPA a real system is replaced by an ordered lattice of effective scatterers. The properties of these effective atoms have to be determined self-consistently from the condition that the scattering of electrons off the alloy components embedded in the effective medium as impurities vanishes on the average. The key quantity in the calculation is the one-electron auxiliary Green's function, and the CPA is an excellent approximation for calculating its average value in random alloys.<sup>44</sup> The accuracy of the CPA for total energy calculations of Fe-based alloys was recently demonstrated in Ref. 45.

However, because of the mean-field nature of this approximation, certain quantities cannot be investigated. In particular, in most of the theoretical works on FeNi alloys the emphasis is put on the average properties of the alloy. At the same time, one of the main distinctions between an ordered and a disordered system is the existence of local environment effects. In an ideally ordered periodic solid all atoms that occupy equivalent positions in the crystal unit cell have exactly the same properties. In a disordered system all chemically equivalent atoms are, strictly speaking, different. The presence of these so-called local environment effects has been largely ignored in earlier theories of the Invar effect. For example, the CPA neglects them completely.

In order to overcome this difficulty, and to investigate the effects of the local environment on the properties of the FeNi system, we model the random binary alloy around the Invar composition by a supercell, constructed following the methodology introduced by Zunger *et al.* for the so-called special quasirandom structures (SQS).<sup>46</sup> This is done by occupying sites of the supercell constructed on the fcc underlying lattice by Fe or Ni atoms in such a way that the Warren-Cowley short range order (SRO) parameters are equal to zero for at least the first four coordination shells.

### B. Exact muffin-tin orbitals—CPA calculations

For the CPA calculations we used the Green's function implementation<sup>47–49</sup> of the *exact muffin-tin orbitals* (EMTO) theory,<sup>50–53</sup> combined with the full charge density (FCD)<sup>54,55</sup> technique. An implementation of the method for random alloys is described in Ref. 37. One of the main advantages of the EMTO theory is the use of optimized overlapping muffin-tin (OOMT) potentials, which can be constructed directly from the full potential. This provides an accurate representation of the one-electron potential. As an output from EMTO calculations one obtains the self-consistent auxiliary Green's function and one-electron states, and as a final result one reconstructs the complete nonspherical one-electron density. The total energy is calculated using the full charge density (FCD) method with the shape function technique,<sup>54,55</sup>

which is utilized to integrate the density over a unit cell. For the EMT0-CPA calculations we used the generalized gradient approximation with the Perdew, Burke, and Ernzerhof (PBE)<sup>33</sup> parametrization of the exchange and correlation functional. The calculations for all spin spirals were performed with 3375  $k$ -points in the irreducible wedge of the Brillouin zone, distributed with the Monkhorst-Pack routine.<sup>56</sup> For the antiferromagnetic structure and for the double layer antiferromagnetic phase, 1800  $k$ -points and 252  $k$ -points, respectively, were used in the irreducible wedge and were also distributed with the Monkhorst-Pack routine. For the ferromagnetic structure, 1505  $k$ -points were used and for the DLMs and the nonmagnetic phases, 916  $k$ -points were distributed uniformly over the irreducible wedge. The calculations were converged in energy with respect to  $k$ -points to an accuracy of around 0.02 mRy.

### C. Projector augmented-wave supercell calculations

To generate a supercell with the required properties of the correlation functions mentioned above, we make use of a Metropolis-like algorithm.<sup>57</sup> The  $N_k$  correlation functions which we want to match determine a vector  $\xi$  in an  $N_k$ -dimensional space. Starting from an arbitrary initial configuration corresponding to some vector  $\xi'$ , a particular pair of atoms of different kinds, chosen at random, are considered and a vector  $\xi''$  corresponding to an exchange of the two atoms is calculated. If the distance in the  $N_k$ -dimensional space between  $\xi''$  and  $\xi$  is less than the distance between  $\xi'$  and  $\xi$ , the exchange is accepted, otherwise the initial configuration is kept. The procedure is repeated until we have generated a configuration sufficiently close to the one required.

We have constructed two supercells with Ni composition around 35 at. %, with 64 and 96 atoms, respectively. The solution of the electronic structure problem for the supercells was carried out by means of the projector augmented-wave (PAW) method<sup>38</sup> as implemented in the Vienna *Ab Initio* Simulation Package (VASP).<sup>39,40</sup> Exchange and correlation effects were treated in the framework of the generalized gradient approximation (GGA) using both the parametrizations by Perdew and Wang<sup>32,58</sup> and by Perdew, Burke, and Ernzerhof.<sup>33</sup> The energy cutoff for the plane waves was equal to 267.91 eV, respectively 269.53 eV for 64- and 96-atom supercells. The integration over the Brillouin zone was done on  $k$ -points distributed according to the Monkhorst-Pack scheme.<sup>56</sup> The number of  $k$ -points was equal to 16. We considered collinear magnetic configurations, although spin flips were allowed.

## III. ANALYSIS OF THE APPROXIMATIONS INVOLVED IN THE SIMULATIONS OF THE FENI ALLOYS

In this work we deal with a problem where complex magnetism is deeply interconnected with chemical disorder in the system. Obviously, our treatment involves modeling of real FeNi alloys using approximations, though our goal is to consider as realistic a system as possible. Still, before we present our results, we would like to analyze our model system and

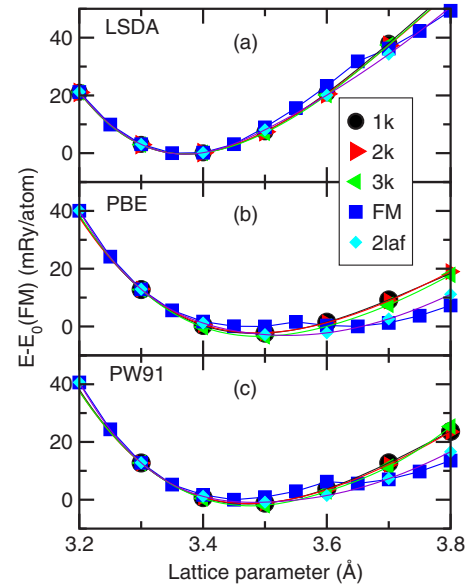


FIG. 1. (Color online) Total energy calculated by means of the PAW technique for different magnetic states of pure fcc Fe as a function of the lattice parameter within three different approximations for the exchange correlation potential and one-electron energy, (a) the local spin density approximation, LSDA (Ref. 35), the generalized gradient approximation using the parametrizations of (b) Perdew, Burke, and Ernzerhof (PBE) (Ref. 33) and of (c) Perdew and Wang (PW91) (Ref. 32), respectively. Considered here are the ferromagnetic order of magnetic moments (filled squares), a collinear antiferromagnetic state, with magnetic moments ordered parallel to each other within (001) planes, but antiparallel to the moments in each nearest plane (1k state, solid circles), a double layer antiferromagnetic state along the (001) direction (diamonds), and two non-collinear states, the so-called 2k (right triangles) and 3k (left triangles) states, described, e.g., in Ref. 22.

make it clear for the readers which approximations are involved, and what possible consequences these approximations can have. Below we consider four levels of our model, that is, a treatment of the exchange and correlation effects, an approximation for the shape of the one-electron potential and magnetization density, a limit on the symmetry of magnetic states considered, and the structural model of the alloys adopted in this study.

### A. Influence of the exchange and correlation functional on the magnetic structure of pure fcc Fe

In Fig. 1 we show results of our calculations carried out for selected sets of magnetic states in pure fcc Fe using different approximations for the exchange-correlation energy and one-electron potential. The results are obtained by means of the PAW technique. We considered the ferromagnetic order of magnetic moments, which led to a high-spin (HS) state at large values of the lattice parameter, and to a low-spin (LS), nearly nonmagnetic state at smaller lattice parameters. This general behavior of the total energy on volume for the ferromagnetic solution is in agreement with earlier studies.<sup>20,27,28,59-69</sup> We also included a collinear antiferromagnetic state, with magnetic moments ordered parallel to

each other within (001) planes, but antiparallel to the moments in each nearest plane (the so-called  $1\mathbf{k}$  state), as well as the double layer antiferromagnetic state along the (001) direction. Moreover, we considered two noncollinear states, the so-called  $2\mathbf{k}$  and  $3\mathbf{k}$  states, described, e.g., in Ref. 22.

Different panels in Fig. 1 show the total energies for different magnetic states of the pure fcc Fe as a function of the lattice parameter within three different approximations for the exchange correlation potential and one-electron energy: Fig. 1(a) shows the local density approximation, LSDA,<sup>35</sup> Fig. 1(b) shows the generalized gradient approximation using the parametrizations of Perdew, Burke, and Ernzerhof,<sup>33</sup> and in Fig. 1(c) of Perdew and Wang,<sup>32</sup> respectively. Similar to the results of earlier studies,<sup>19–23</sup> we can see that there exists a competition between a large number of magnetic states, with different states stable at different volumes. In Ref. 7 this was explained by a competition between a tendency toward long range (ferromagnetic or antiferromagnetic, depending on the lattice parameter) order due to the nearest-neighbor exchange interaction and a tendency toward a spin-glass-like state due to oscillating behavior of the more distant exchange interactions, which cancel each other's contribution to the effective exchange parameter almost exactly.

We will analyze the particular order of the states and compare our results with other works in more detail in the next section. What we would like to emphasize now is that though the general trends seen in three panels of Fig. 1 are rather similar, the detailed behavior of the curves is different between the different approximations for exchange and correlation. While it is well recognized by now that magnetic structures calculated by the LSDA and the GGA in transition metals can be different, we find that even *within* the GGA, different parametrizations of the functional produce rather different results. Indeed, if one pays attention, for instance, to the difference between the energy minima for the HS and the LS ferromagnetic states, one sees that the two are essentially degenerate for the PBE functional, while the latter has lower energy for the PW parametrization. We note in passing that our PW results for the energy difference between the HS and LS FM states are in excellent agreement with calculations by Sjöstedt and Nordström,<sup>22</sup> while our PBE results agree well with those reported by Knöpfle *et al.*<sup>21</sup> We thus can speculate that different parametrizations of the exchange correlation functional were used in these studies.

The observation above suggests that it might be impossible to predict the exact magnetic ground state of an Fe-based alloy for, say, a particular composition and volume with the present day level of first-principles calculations based on currently available local exchange-correlation functionals. Indeed, even for pure Fe theoretical works fail to reproduce the experimental magnetic structure observed for fcc precipitates in Cu. As was discussed in the Introduction, even perhaps the most accurate calculations by Sjöstedt and Nordström<sup>22</sup> reproduce the experimentally observed ordering vector of the spin spiral only at values of the lattice parameter which are smaller than that of Cu. In any case, there is no way to validate the results presented in Fig. 1 on the basis of available experimental information. In this sense it would be very interesting to apply novel methodologies, e.g., the dynamical mean field theory (DMFT),<sup>70,71</sup> for the investiga-

tion of magnetic properties of fcc Fe and Fe-based alloys. As a matter of fact, the DMFT calculations were carried out for bcc Fe.<sup>72–74</sup> Moreover, recently Minar *et al.*<sup>75</sup> have tested the technique for fcc Fe-Ni alloys, and showed that the DMFT calculations did not spoil the overall behavior for the concentration dependence of magnetic moments as compared to conventional LSDA simulations. An extension of such studies toward the investigation of the total energy and complex magnetic structures is highly motivated.

Summarizing the above arguments, we decide to concentrate on the investigation of the trends, which may be reliably calculated within the LSDA or GGA approach, and to study general features of the evolution of magnetic structures as a function of composition in FeNi alloys. As a practical tool, we use mostly the PBE-GGA parametrization, which means that the stability of our ferromagnetic solution is perhaps somewhat overestimated, at least with respect to the calculations which use LSDA and PW. Because most of the earlier studies of FeNi alloys were carried out within the LSDA,<sup>5,16,20,27,28</sup> which could have somewhat overestimated the stability of the LS and/or noncollinear solutions, we are able to establish upper and lower bounds on the predictions of the theoretical magnetic ground state of the alloys.

## B. Spherical cell approximation for the one-electron potential

During the self-consistent iterations with the EMTO method, the one-electron potential is assumed to be spherically symmetric within the so-called potential spheres centered at the positions of the ideal underlying crystal lattice. Large overlaps between the potential spheres are allowed, because they are treated exactly, and the construction of the spherical potentials is optimized to give the best possible representation to the full (nonspherical) crystal potential. Moreover, the self-consistent iterations within this so-called spherical cell approximation are complemented with the full charge density calculations of the total energy. The accuracy of the FCD calculations as well as the accuracy of the EMTO in general is also provided by correct normalization of the electronic state within the WS cell. This gives the EMTO-FCD method the reliability comparable to state-of-the-art full potential methods.<sup>45</sup>

In Fig. 2 we demonstrate this explicitly, by showing the total energies as a function of lattice parameter calculated for different magnetic states in pure fcc Fe. We show results for the nonmagnetic and ferromagnetic (HS and LS) states,  $1\mathbf{k}$  and double layer antiferromagnetic (AFM) states, as well as for the spin spiral state. The latter corresponds to the planar spin spiral with the wave vector along the  $\Gamma$ -X direction in the Brillouin zone which minimize the total energy for the spin spiral (see inset in Fig. 2). This state was considered in earlier studies of the noncollinear magnetism in fcc Fe.<sup>21,22</sup> We also show total energies of the so-called partial disordered local moment (PDLM) state<sup>26,76</sup> simulated by means of a system with different fractions of randomly distributed spin up and spin down atoms.

In the EMTO calculations we use the PBE parametrization for the exchange and correlation functional, and therefore in order to verify the accuracy of this method with re-

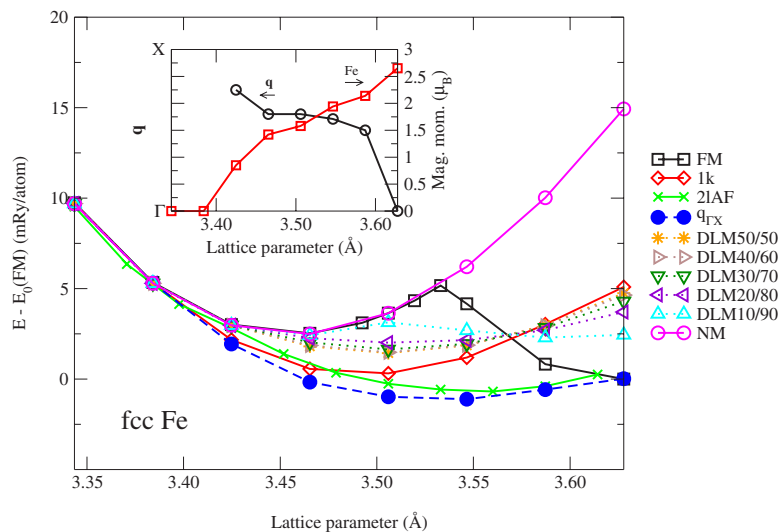


FIG. 2. (Color online) Total energies calculated by means of the EMTO method for different magnetic states of pure fcc Fe as a function of the lattice parameter within the generalized gradient approximation using the parametrization of Perdew, Burke, and Ernzerhof (Ref. 33). Shown are results for the nonmagnetic (open circles, solid line) and ferromagnetic states (open squares, solid line),  $1\mathbf{k}$  (diamonds) and double layer ( $X$ , solid line) AFM states, as well as for the spin spiral state (filled circles, dashed line). The latter corresponds to the planar spin spiral with the wave vector  $q$  along the  $\Gamma$ - $X$  direction in the Brillouin zone which minimizes the total energy for the spin spiral. The dependence of the wave vector  $q$  and magnetic moment for the spin-spiral state on the lattice parameter is shown in the inset in the figure. Also shown are the total energies for the partial disordered local moment states (dotted lines) with a relative fraction of the spin-down component 10 (triangles up), 20 (triangles left), 30 (triangles down), 40 (triangles right), and 50 % (stars).

spect to the full-potential PAW calculations the results shown in Fig. 2 must be compared to those in Fig. 1(b). One can see excellent agreement between two sets of calculations with respect to the relative stability of different magnetic states, as well as transition volumes between different states.

As a matter of fact, the agreement between the two sets of calculations serves not only as a justification of the accuracy of the spherical cell approximation adopted within the EMTO method, but also as a justification of the PAW calculations. Indeed, the EMTO method is a truly all-electron technique, while the PAW methodology still involves pseudopotentials. PAW potentials of Fe are known to be reliable, and our calculations confirm this conclusion. In summary, we have shown that two different techniques, the EMTO and PAW methods, produce consistent results for the magnetic structure of pure fcc Fe, and we can use this complementarity in our studies of the alloys.

### C. Atomic moment approximation for the magnetization density and motivation for the choice of magnetic states

In order to determine the magnetic ground state for the FeNi alloys from first principles rigorously, one strictly speaking has to run simulations for infinitely large system (to allow for the incommensurate states in chemically disordered material), to include the effects of inter- as well as intra-atomic noncollinearity similar to Refs. 21 and 22, to relax the magnetic structure during the self-consistent iterations,<sup>16,19,29</sup> as well as to account for local displacement of ions off their ideal lattice sites,<sup>77</sup> and to consider possible effects due to chemical short-range order.<sup>5</sup> Such simulations do not seem to be feasible, and besides, inaccuracies in the

underlying local approximations for the exchange and correlation potentials discussed in Sec. III A do not allow us to study anything but trends anyhow. In this study we therefore adopt a number of approximations on the magnetization density and on the symmetry of magnetic states considered.

We use the spherical cell approximation in our EMTO calculations, and we treat the magnetization density within the atomic moment approximation, neglecting therefore the effect of intra-atomic noncollinearity. In our PAW calculations we also use the atomic moment approximation for the magnetization density. Moreover, the symmetry of a magnetic state is defined as an input parameter, and is not modified during the self-consistency cycle. Because it is impossible to explore all symmetries of complex magnetic solutions by the constrained calculations, we have to choose carefully the magnetic states which are considered. In this work we carry out total energy calculations for the nonmagnetic and ferromagnetic (HS and LS) states,  $1\mathbf{k}$ , and double layer AFM states, as well as for the planar spin spiral with wave vector along the  $\Gamma$ - $X$  direction in the Brillouin zone. Also we include the partially disordered local moment states with a relative fraction of the spin-down component 10, 20, 30, 40, and 50 %. This means that, for instance, the PDLM state with equal fraction of spin-up and spin-down components in the  $\text{Fe}_{70}\text{Ni}_{30}$  alloy is simulated as an effective four component alloy  $\text{Fe}_{35}^{\uparrow}\text{Fe}_{35}^{\downarrow}\text{Ni}_{15}^{\uparrow}\text{Ni}_{15}^{\downarrow}$ . It has been shown before that the above mentioned state represents very well the total energy of the paramagnetic alloy above the Curie temperature.<sup>78,79</sup> The importance of the PDLM states for the description of the ground state magnetic structure of the FeNi Invar alloys was also stressed in Refs. 5, 24, and 26, so we consider them here as well.

In general, our choice of magnetic states is motivated by earlier studies of the noncollinear magnetism in fcc Fe and collinear magnetism in FeNi alloys. In particular, we should note that we did not perform calculations for the low moment  $X$ - $W$  spin spiral (which actually is the experimental ground state structure of fcc Fe). For fcc Fe the difference in energy between the  $\Gamma$ - $X$  and  $X$ - $W$  spin spirals is about 0.02 mRy, which is beyond the accuracy in which we are interested in this work. Moreover, we do not expect the  $X$ - $W$  spin spiral state to be stabilized by alloying with Ni. Indeed, in pure Fe it is stabilized at low volumes, according to Refs. 21 and 22. On the contrary, in the alloys, as will be shown below, the magnetic ground state moves toward higher volumes, and states closer to the  $\Gamma$  point become more stable. Thus we believe that the  $X$ - $W$  spin spiral is not interesting for the alloys, where there is always some other structure lower in energy. This conclusion is supported by calculations carried out by Kissavos<sup>80</sup> using the Korringa-Kohn-Rostoker (KKR) method within the atomic sphere approximation. Also, we do not consider the  $2\mathbf{k}$  or  $3\mathbf{k}$  noncollinear structures. As one can see in Fig. 1, the  $2\mathbf{k}$  state turns out to be the ground state structure at lower volumes in our PAW simulations for fcc Fe. However, in Ref. 22 this is shown to be a possible artifact of the atomic moment approximation for the magnetization density, and the  $1\mathbf{k}$  AFM state has lower energy when the intra-atomic noncollinearity is included. The energy difference between these two states is rather small, and the addition of Ni destabilizes them strongly with respect to other magnetic states. We therefore decided to represent the family of these three states,  $1\mathbf{k}$ ,  $2\mathbf{k}$ , and  $3\mathbf{k}$  by the simplest one, the  $1\mathbf{k}$  state. Similarly, we do not consider either the triple layer AFM state or four layer AFM state along (001) direction. In Ref. 20 these states were found to be competing with the double layer AFM and the ferromagnetic (FM) states at large volumes, being very close in energy to the former. We will show in this paper that there are other magnetic states more important than the double layer AFM state in the region of the transition to the FM state. We thus represent the family of multilayer AFM states by a double layer solution.

Finally, it is well known that particular care needs to be taken to describe the LS FM state. In many cases one has to carry out the so-called fixed spin moment calculations in order to obtain very well converged results.<sup>63,64</sup> However, with respect to other magnetic states, the transition between the HS and the LS FM states occurs at higher energies, see Figs. 1 and 2. Therefore we carry out conventional floating moment calculations for all the magnetic states at all volumes, and neglect possible very small (see, e.g., Fig. 1 in Ref. 21) errors in the total energy of the states in the region of the HS to LS transition.

#### D. Structural model

Let us now comment on the structural model which we adopt for the FeNi alloys in this study. For all compositions we consider a completely random distribution of atoms at the sites of the ideal undistorted fcc crystal lattice. In principle, the experimental phase diagram, as well as theoretical

studies<sup>5,81</sup> show the existence of ordering trends in the FeNi alloys, and their possible importance for the understanding of the Invar effect. On the other hand, theoretical simulations,<sup>81</sup> in agreement with experimental studies,<sup>82</sup> show that the short range order parameters in FeNi alloys actually are rather small, and therefore the ordering effects cannot account for, for instance, the existence of the Invar effect itself. Thus we neglect the effects of short-range order in this study. This is of course a relevant and interesting subject on its own, and we will investigate it in the future.

The experimental studies also show that the relative changes of mean nearest neighbor interatomic distances due to local lattice relaxations in FeNi alloys are small ( $\leq 0.6\%$ ).<sup>82,83</sup> Liot *et al.*<sup>77</sup> have studied individual nearest neighbor interatomic distances for the random fcc Fe<sub>50</sub>Ni<sub>50</sub> alloy with a lattice constant equal to 3.588 Å, which is very close to the experimental lattice constants. According to the calculations, the changes of the average bond lengths between Fe-Fe, Fe-Ni, and Ni-Ni ions due to local lattice relaxations are relatively small. However, for all types of pairs the dispersion of the interatomic distances is rather large compared to the changes of the average distances. The influence of static ionic displacements on the local magnetic moments at individual sites in the alloy was also investigated. It turned out to be very small. We therefore neglect the effect of local lattice relaxations for most calculations presented in this work. However, for selected cases the positions of atoms in the supercell will be relaxed. A complete investigation of the influence of the atoms displacements off the sites of the ideal fcc lattice on the properties of FeNi alloys will be presented elsewhere.

#### IV. MAGNETIC STRUCTURE OF FENI ALLOY AS A FUNCTION OF COMPOSITION

Let us start our description of the FeNi alloys with a consideration of pure fcc Fe, Fig. 2. The results obtained by the EMT method show familiar trends. At low volumes the AFM solution is more stable, followed by the spin spiral solution at larger volumes. The latter transforms into the DL AFM solution with further increase of the lattice constant. Finally, at large volumes the HS FM solution is stabilized. The competition between different magnetic states in pure fcc Fe is associated with a competition between a tendency toward long range order due to the nearest-neighbor exchange interaction, which changes sign from AFM to FM with increasing volume passing through zero, and a tendency toward a formation of a spin-glass-like state due to oscillating behavior of the more distant exchange interactions, which cancel each other's contributions to the effective exchange parameter almost exactly.<sup>7,30</sup>

In comparison to earlier LSDA calculations, the relative stability of the HS FM state is much higher. For instance, it is lower in energy than the LS FM state, and if we neglect the AFM states, similar to earlier studies of Invar alloys, we would conclude that the HS FM should be the ground state of fcc Fe. Interestingly, the DLM states do not compete with ordered magnetic states at any value of the lattice parameter; they are always rather high in energy. This in particular

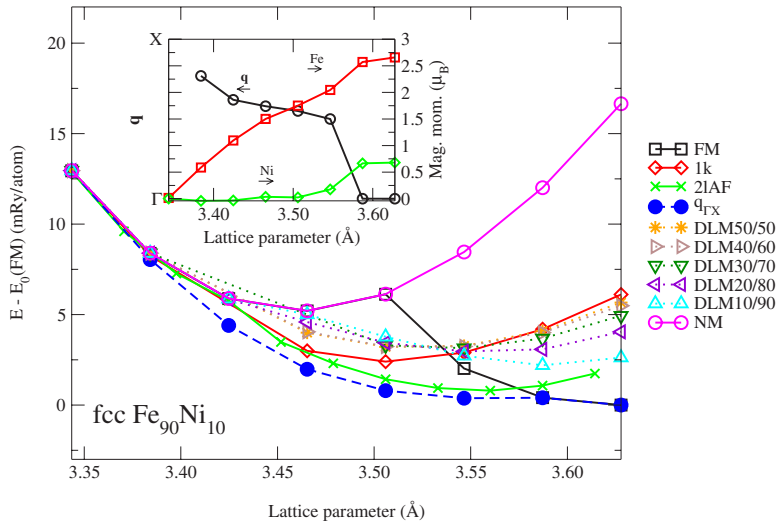


FIG. 3. (Color online) Total energies calculated by means of the EMTO method for different magnetic states of the fcc  $\text{Fe}_{90}\text{Ni}_{10}$  alloy as a function of the lattice parameter. Notations are the same as in Fig. 2.

means that the temperature of real magnetic disorder in fcc Fe could be relatively high. However, one should not expect to see this easily, for instance, from the measurements of the net magnetization or with Mössbauer spectroscopy, as it might be difficult to distinguish between the real paramagnetic state, and a mixture of antiferromagnetic states which are all close in energy, and therefore could be excited in the system at elevated temperatures.

When Ni is added to the system, the evolution of the magnetic structure is generally characterized by an increased stability of the FM solution, and a shift of the magnetic phase transition toward lower volumes. In Figs. 3–8 this is illustrated directly by our total energy calculations. Already in the alloy with 10 at. % Ni we see substantial modifications in the behavior of the binding energy curve, Fig. 3. Indeed, the AFM solutions destabilize, while the spin spiral solution and the FM solution become more stable. As a matter of fact, these are the only two solutions that describe a transition from the LS state to the HS state within the mean-field approximation to the chemical disorder. The AFM, DL AFM, and PDLM solutions are not stable at any value of the lattice parameter. The trend becomes more clear with increasing Ni concentration, Figs. 4–8. It is interesting to point out that the

energy difference between different magnetic states considered in this study decreases in the transition region with increasing fraction of Ni, but the transition region itself shifts to higher energies with respect to the ground state magnetic structure at the particular composition.

This picture agrees well with an observation made in Ref. 30, where the so-called effective exchange parameter  $J_0$  of the classical Heisenberg Hamiltonian for magnetic interactions was studied in face-centered cubic (fcc) metals as a function of volume and occupation of the valence band across 3d transition metal series, from Mn to Ni. It was found that there exists a valley in the volume–electron concentration phase space, where the effective exchange parameter varies drastically, indicating very strong dependence of the alloy magnetic structure on the composition. The FeNi alloys considered here are exactly in this area of volumes and electron concentrations, and their magnetic states are extremely sensitive to the fraction of Ni, as is indeed shown in Figs. 3–8.

We can summarize a picture which emerges from our EMTO-CPA calculations. They show that there is a transition region from the LS state to the HS FM state. In the transition region there are many magnetic states with total energies

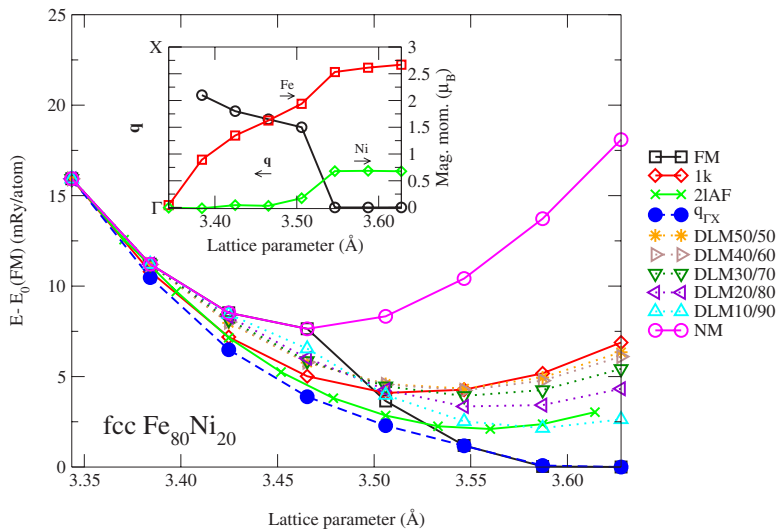


FIG. 4. (Color online) Total energies calculated by means of the EMTO method for different magnetic states of the fcc  $\text{Fe}_{80}\text{Ni}_{20}$  alloy as a function of the lattice parameter. Notations are the same as in Fig. 2.

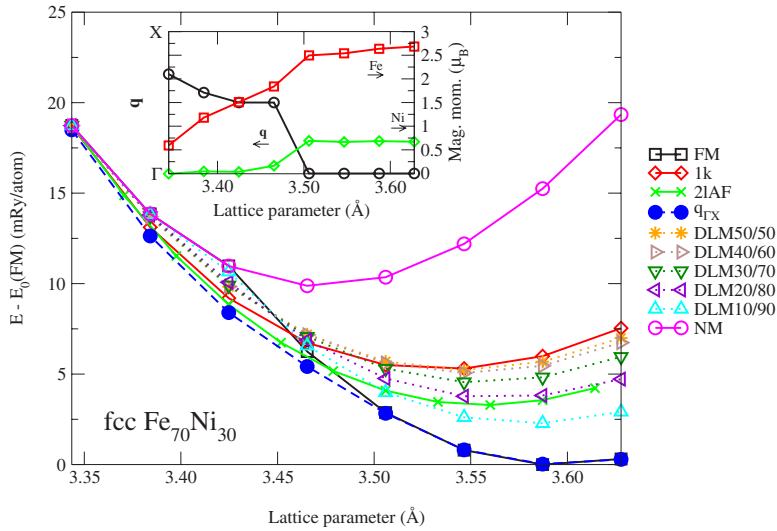


FIG. 5. (Color online) Total energies calculated by means of the EMTO method for different magnetic states of the fcc  $\text{Fe}_{70}\text{Ni}_{30}$  alloy as a function of the lattice parameter. Notations are the same as in Fig. 2.

close to each other. The region shifts off the equilibrium volume toward lower volumes with increasing Ni concentration. This is in agreement with an observation of the pressure induced Invar effect in FeNi alloys.<sup>8</sup> The FM state is stable for most of the compositions. As a matter of fact, its stability range is much larger than in earlier LSDA calculations. PDLM results do not compete with other configurations either, so earlier works which emphasize the importance of the PDLM and DLM states for Invar alloys<sup>24,26</sup> are not supported by the present study. The most important competing magnetic state is the spin spiral state. But in PBE-GGA simulations even this structure is too far away from the equilibrium volume at Invar composition, see Fig. 6. One may therefore ask a question if the magnetic phase transition is relevant for the understanding of the ground state magnetic structure of Fe-Ni Invar alloys. In order to answer this question, we need to go beyond the mean-field picture of the chemical disorder in the system.

**V. MAGNETIC STRUCTURE OF THE  $\text{Fe}_{65}\text{Ni}_{35}$  ALLOY FROM SUPERCELL CALCULATIONS**

In Ref. 16 van Schilfgarde *et al.* investigated the evolution of magnetic structures in FeNi Invar alloys as a function

of unit cell volume. It was observed that at a volume per atom  $\Omega = 75.7$  a.u., two Fe spins made a discontinuous transition from the FM configuration to an approximately anti-ferromagnetic alignment with slightly reduced local moments. These spin flips catalyzed the transition to a noncollinear alignment for smaller lattice constants. Thus one possible magnetic configuration, not included in the EMTO-CPA simulations, may be a ferrimagnetic state with several local moments at Fe atoms pointed antiparallel to the net magnetization direction. We will call this configuration as a spin flip (SF) configuration.

In a subsequent study by Ruban *et al.*<sup>7</sup> it was observed that in the  $\text{Fe}_{50}\text{Ni}_{50}$  alloy the so-called effective exchange parameters  $J_0$  of the classical Heisenberg Hamiltonian depend strongly on the local chemical environment of the atoms, that is, on the number of unlike nearest neighbors in the first coordination shell of each atom in the alloy. At large volumes the difference was found to be negligible. But with decreasing volume the exchange parameters at Fe atoms in different chemical environments rapidly decreased, while the difference between them increased. In particular, they crossed zero line at different volumes. Because  $J_0$  as calculated in that work indicated a tendency of the spin at a particular site to rotate from its original direction in the ferro-

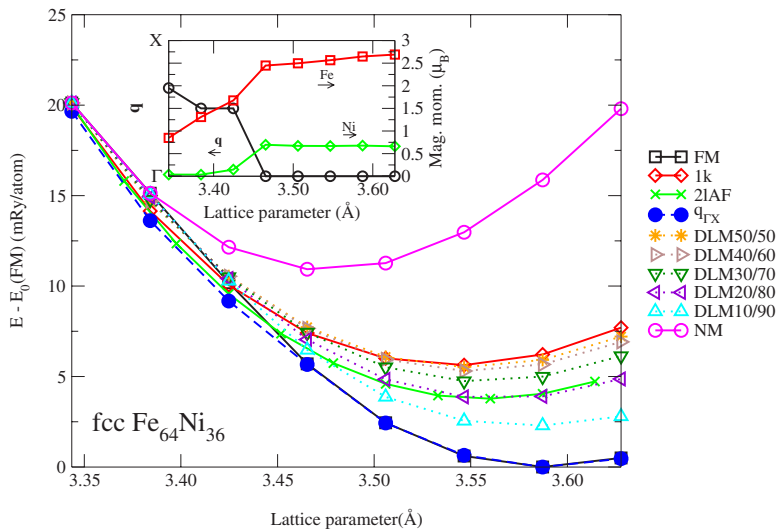


FIG. 6. (Color online) Total energies calculated by means of the EMTO method for different magnetic states of the fcc  $\text{Fe}_{64}\text{Ni}_{36}$  alloy as a function of the lattice parameter. Notations are the same as in Fig. 2.

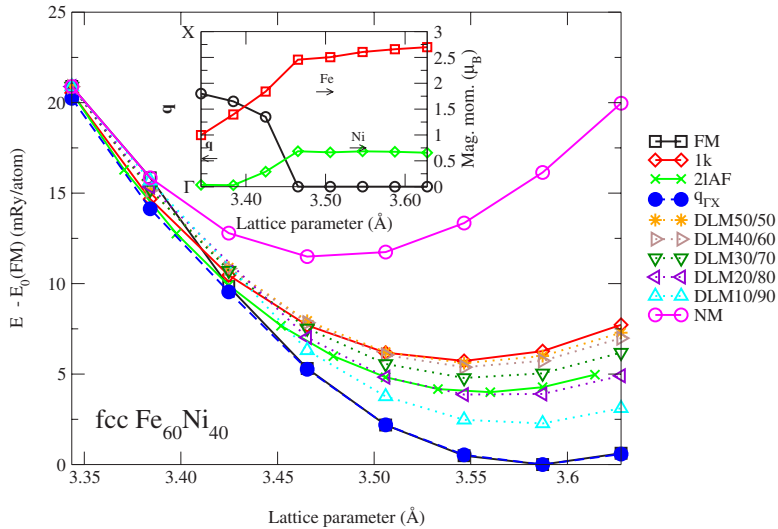


FIG. 7. (Color online) Total energies calculated by means of the EMTO method for different magnetic states of the fcc  $\text{Fe}_{60}\text{Ni}_{40}$  alloy as a function of the lattice parameter. Notations are the same as in Fig. 2.

magnetic system, Ruban *et al.* concluded that this tendency differs substantially between different atoms in the alloy, being stronger for Fe atoms with more Fe neighbors. This conclusion agrees with the above mentioned observation made by van Schilfgarde *et al.*,<sup>16</sup> and suggests that the spin flip configuration can compete with either the FM or the spin spiral magnetic state in Invar alloys. Abrikosov *et al.*<sup>31</sup> also observed the spin flip transition in the equiatomic alloy in their supercell calculations using the KKR-ASA method.

It is important to note that all the works mentioned above simulated the FeNi alloys within the LSDA, and did not include the possibility of a spin spiral solution. Besides, Refs. 7 and 31 considered an equiatomic alloy rather than an Invar alloy. In order to investigate the relative stability of the SF configuration with respect to other low-energy magnetic excitations considered in this work, we carried out PAW calculations for the  $\text{Fe}_{65}\text{Ni}_{35}$  alloy modeled as a supercell with 96 atoms randomly distributed at the sites of the underlying fcc crystal lattice in such a way that the Warren-Cowley SRO parameters are equal to zero for at least the first four coordination shells; see Sec. II C. In these simulations we considered only collinear states, ferromagnetic, spin flip, and

double layer AFM (the 1k AFM state is higher in energy than the DL AFM state at all values of the lattice parameter, which are of interest, see Fig. 6). However, based on the good agreement between our EMTO and PAW calculations, as discussed in Sec. III B, we are also able to draw conclusions on the relative stability of these states with respect to the spin spiral state.

Our simulations show that the ground state magnetic structure of  $\text{Fe}_{65}\text{Ni}_{35}$  is FM, with an equilibrium lattice parameter of 3.59 Å. We are able to stabilize the SF and DL AFM at lower volumes. In agreement with the analysis of the dependence of the exchange parameters on the number of unlike and like nearest neighbors,<sup>7</sup> the spin flip occurs at an Fe site surrounded by the largest number of Fe atoms in our supercell, which was the site with 11 Fe neighbors out of 12. We find that at a lattice parameter of 3.52 Å, the SF configuration is nearly degenerate with the FM state. The DL AFM state is 2.35 mRy higher in energy at this volume. As a matter of fact, here we also tested a triple layer AFM state along the (001) direction, which was found to compete with the FM state at large volumes in Ref. 20. Indeed, it turns out to be 0.43 mRy more stable than the DL AFM state, but still

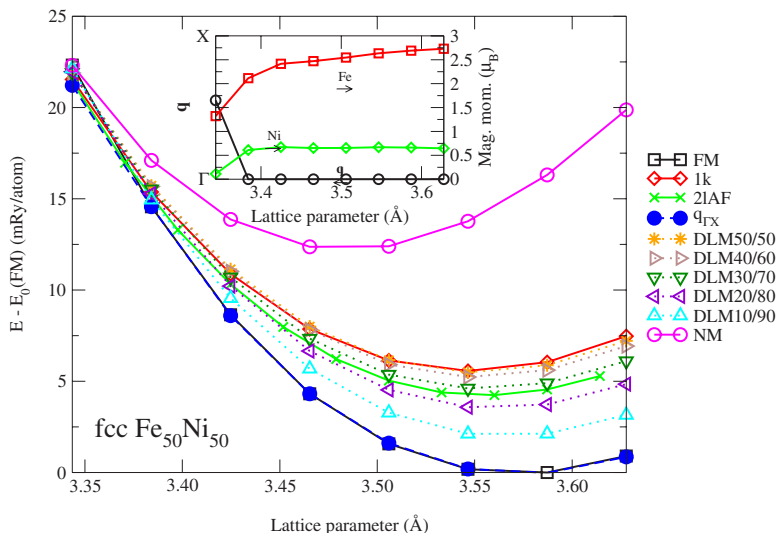


FIG. 8. (Color online) Total energies calculated by means of the EMTO method for different magnetic states of the fcc  $\text{Fe}_{50}\text{Ni}_{50}$  alloy as a function of the lattice parameter. Notations are the same as in Fig. 2.

less stable than either the FM or the SF states.

We did not calculate the total energy of the spin spiral state for the supercell directly, but from Fig. 6 we see that it becomes more stable than the FM state at a lattice parameter of 3.45 Å. Now, we have shown earlier in Sec. III B that the EMTO and PAW calculations are complimentary to each other, in particular the lattice parameter of the FM Fe<sub>65</sub>Ni<sub>35</sub> alloy (3.59 Å) and the energy difference between the FM and the DL AFM states at the lattice parameter of the spin flip transition (about 2.3 mRy at 3.52 Å) agree very well between the PAW and EMTO-CPA calculations. Thus we can compare transition volumes for different magnetic states obtained by the two different methods, and we conclude that the SF transition occurs closer to the equilibrium volume compared to a transition from the FM to the spin spiral state. We therefore confirm the conclusion of Ref. 16 that the (nearly) collinear SF state could be the closest in energy magnetic state to the FM configuration in Invar alloys.

However, there is one important difference between our results and the simulations presented in Ref. 16. In the latter work the spin flip transition occurs at a volume which is larger than the theoretical equilibrium volume for the alloy, and therefore the predicted ground state corresponds to a weakly noncollinear ferromagnetic state. In the present case we observe that the transition takes place at compressed volumes, and the lowest energy configuration is ferromagnetic. This is due to the different approximations to the exchange and correlation functional used here (PBE-GGA) and in Ref. 16 (LSDA). Unfortunately, as was discussed in Sec. III A it is impossible to discriminate between different approximations, GGA and LSDA, on the basis of available experimental information. Thus it seems to be impossible to exactly predict the magnetic ground state of Fe-based alloys for a particular composition and volume with the current approximations involved in the density functional theory calculations. The trends observed in either LSDA or GGA simulations are clearly similar though, namely, the SF state is predicted to be the first in a series of magnetic transitions in the FeNi alloy upon compression of the material from the high-spin ferromagnetic state at large volumes toward smaller volumes.

To investigate this point in more detail, we carried out PAW calculations for the Fe<sub>65</sub>Ni<sub>35</sub> alloy using a smaller supercell of 64 atoms and the PW-GGA parametrization for the exchange and correlation energy functional. In these simulations we include only the SF and FM configurations. Our results are shown in Fig. 9(a). One can clearly see that the SF transition takes place as well, but at the lattice parameter 3.55 Å, which is closer to the equilibrium as compared to PBE-GGA calculations.

In the case of the 64-atom supercell, we have checked the influence of the local displacements of ions off the sites of the ideal fcc lattice. The dependence of the total energy for the FM and SF states on the lattice parameter for the fully relaxed supercell is shown in Fig. 9(b). As expected, the influence of the local relaxations is found to be almost negligible, though it shifts the transition slightly toward larger volumes. Note also that in the 64-atom supercell the largest Fe cluster consisted of a central Fe site with nine Fe nearest neighbors. The spin flips at the central site of the cluster, in

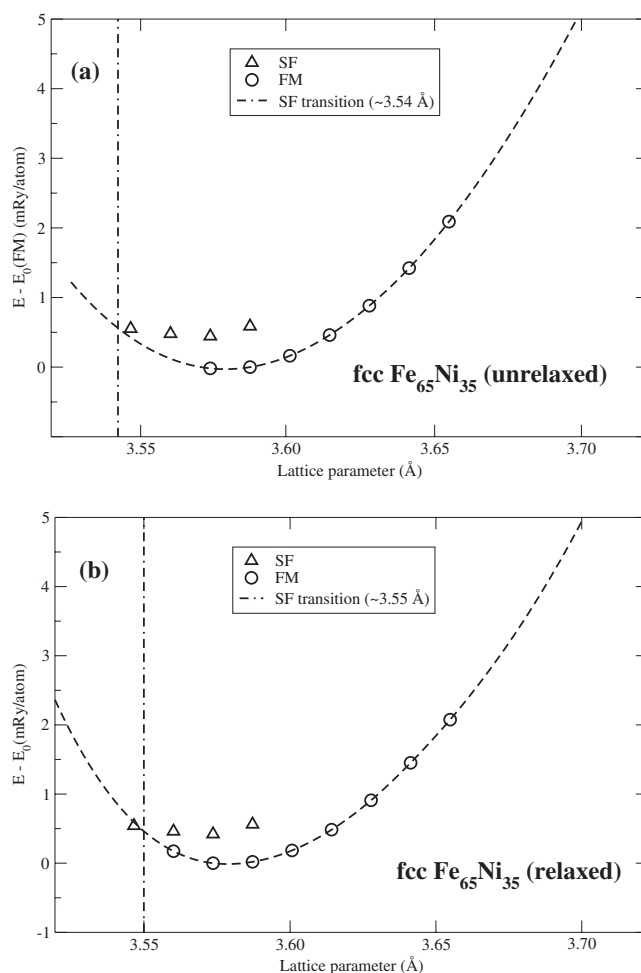


FIG. 9. Total energy calculated by means of the PAW technique for the spin flipped (SF, triangles) and ferromagnetic (FM, circles, dashed line) magnetic states in the Fe<sub>65</sub>Ni<sub>35</sub> alloy as a function of the lattice parameter within the generalized gradient approximation using the parametrization of Perdew and Wang (Ref. 32). The alloy is simulated by a 64-atom supercell with vanishing short-range order parameters up to the fourth coordination shell. In (a) we show results for the calculations where atoms are assumed to be at ideal sites of the fcc underlying crystal lattice. In (b) the results of the calculations for the fully relaxed atomic positions are presented.

agreement with our earlier observation that the SF transition takes place at Fe sites surrounded by the largest number of Fe neighbors. In a real system there will be Fe atoms surrounded by only Fe neighbors though, and one can expect that the transition takes place at even larger volumes, closer to the equilibrium. Thus we conclude that it is quite possible that the ground state of Invar alloys does correspond to a (possibly locally noncollinear) ferrimagnetic state.

At the same time, we would like to underline that the spin flip state is quite different from the partial disordered local moment state considered in Sec. IV. The latter was used as a model of the ground state for Invar alloys in earlier CPA studies.<sup>24,26</sup> The PDLM state modeled by means of the DLM-CPA calculations does not contain any information about the local chemical surrounding of the atoms. That is, the spin flips with equal probability at Fe atoms surrounded

predominantly by Fe, as well as by Ni. The energy cost of the latter transition is higher than for the former. Consequently, the energy of the PDLM state is well above the energy of the FM, SF, and spin spiral states, as is seen in Figs. 2–8.

## VI. DISCUSSION

The results of our simulations clearly illustrate a complexity of the problem related to an identification of the magnetic structure of Fe-Ni alloys in a vicinity of Invar composition. We predict that there is a *family* of magnetic states which are close in energy to each other. While the limitations of the first-principles approach, as discussed above, do not allow for the precise identification of the magnetic structure of the particular alloy at the particular composition and pressure, we can make some general conclusions regarding its evolution. The most important fact is that in contrast to conventional magnetic alloys, the magnetic structure of Fe-Ni Invar alloys depends sensitively on the external parameters.

We predict, in agreement with earlier LSDA calculations,<sup>16</sup> that at large volumes (corresponding to fictitious negative pressure) the Fe<sub>65</sub>Ni<sub>35</sub> alloy is the high-spin ferromagnet. Upon the reduction of volume, the magnetic structure changes. We predict that the FM alloy first transforms into a ferrimagnetic system with local moments on the Fe atoms, which are surrounded by the most Fe neighbors, pointing antiparallel to the direction of the net magnetization. Here we can speculate that these spin flip sites should act as nucleation centers for a formation of spatial regions with complex, most probably noncollinear, magnetic structure inside the ferromagnetic matrix. Upon further compression they should grow until a percolation threshold where the whole system becomes noncollinear. Note that the energy difference between these additional (as compared to the excitations in a conventional ferromagnet) magnetic states in the transition region is extremely small, and they can be thermally excited at relatively low temperatures, e.g., at room temperature. This conclusion is in agreement with well-known anomalous temperature dependence of magnetization in Fe-Ni Invar alloys.<sup>4</sup> Moreover, the number of states available for the system at a fixed temperature *increases* with increasing pressure,<sup>16</sup> and therefore one can expect that the magnetic contribution to a pressure derivative of the system entropy at fixed temperature  $(\partial S_{\text{magn}}/\partial P)_T$  must be positive, at least up to moderate pressures. But according to the Maxwell relation  $(\partial S/\partial P)_T = -(\partial V/\partial T)_P$ , where  $V$  is the volume of the system, one immediately sees that the effect discussed above leads to a *negative* magnetic contribution to the thermal expansion coefficient.

The scenario for the evolution of the magnetic structure in Fe-Ni alloys described above is in line with direct calculations carried out in Ref. 16. Of course, because of the relatively small size of the supercell used in that work it could not capture the effects taking place at large length scale. However, our picture can be supported by several experimental studies carried out recently. The existence of the pressure induced magnetic *phase transition* in fcc Fe-Ni alloy has been unambiguously demonstrated in Refs. 8, 10, 11, and

13. Moreover, Matsushita *et al.*<sup>13</sup> studied magnetic properties of Fe<sub>68.1</sub>Ni<sub>31.9</sub> alloy by ac susceptibility measurements and concluded that their results showed the pressure induced magnetic phase transition from the FM phase to the spin-glass-like high-pressure magnetic phase. Their observation of a reentrant spin-glass-like phase above 3.5 GPa was viewed as an evidence of the coexistence of FM and AFM interactions in the low-temperature region. Wildes and Cowlam,<sup>12</sup> comparing different neutron scattering experiments,<sup>84,85</sup> admitted a possibility of the existence of noncollinear clusters in the ferromagnetic matrix of Fe<sub>65</sub>Ni<sub>35</sub> alloy already at ambient pressure. Willis and Janke-Gilman<sup>15</sup> studied magnetic dichroism in photoemission from Fe-Ni thin film alloys, and observed that within the Invar composition region saturation magnetization showed pronounced deviations from the Slater-Pauling curve, while magnitudes of elemental magnetic moments varied much weaker with concentration, indicating substantial changes in magnetic order for Fe<sub>65</sub>Ni<sub>35</sub> alloy. Foy *et al.*<sup>14</sup> showed the presence of a disorder among Fe moments in Fe-Ni thin film alloys, while Ni moments were aligned in the direction of net magnetization, in agreement with theoretical predictions.

In this sense it is interesting to put our results in the context of earlier theories of the Invar effect. Perhaps the most popular model was due to Weiss<sup>86</sup> who introduced the so-called 2 $\gamma$ -state model. According to this model there are two possible states for  $\gamma$ -Fe (fcc): the ferromagnetic high volume state and the antiferromagnetic low volume state. Thermal excitations between these two states are supposed to compensate for the usual lattice expansion related to anharmonic effects of the lattice vibrations. Recent *ab initio* simulations do agree that the high-spin ferromagnetic state and the low-spin antiferromagnetic state represent the end points of the magnetic phase transition in pure fcc Fe and Fe-Ni alloys (say, as a function of pressure), but they do not support a naive understanding of the Weiss model, according to which the transition occurs between just two states. First-principles simulations clearly identify more than two magnetic states in these systems.<sup>5,6,16,19–24,26</sup>

Although the Weiss picture has been a subject of debate for about half a century, it is still used for the interpretation of the experimental results.<sup>9–11</sup> Indeed, Nataf *et al.*<sup>11</sup> suggested a Weiss-like equation of state and fitted the experimental pressure-volume curve for Fe<sub>64</sub>Ni<sub>36</sub> alloy with this equation. They obtained reasonable quality of the fit, and concluded that the pressure induced phase transition in the alloy lies between 2.5 and 4.5 GPa, in agreement with their earlier conclusion obtained from the studies of the pressure dependence of the bulk modulus.<sup>10</sup> Thus they identify the magnetic state of the Fe<sub>64</sub>Ni<sub>36</sub> alloy at pressure above 4.5 GPa as the low-spin state, that is, the final state for the magnetic phase transition. As a matter of fact, Rueff *et al.*<sup>9</sup> measured Fe magnetization as a function of pressure in the alloy with the same composition, and observed a plateau in the pressure range 5–12 GPa with values of Fe magnetic moments of the order  $0.9 \pm 0.3 \mu_B$ , which was interpreted as due to the fact that the alloy is in the LS state with typical magnetic moment for Fe in the LS state  $0.6 \mu_B$ . However, this conclusion is ambiguous from our point of view. First of all, error bars in Ref. 9 are too large on the scale of the effect

discussed. Second, the use of  $N_2$  pressure medium in the pressure range of the solid-fluid phase transition for the latter, about 2 GPa at 300 K,<sup>87,88</sup> raises questions concerning the hydrostatic pressure conditions in the experiment.

But in any case, the high-pressure experiments in Ref. 9, as well as studies in Ref. 13, carried out for slightly more Fe rich alloy, clearly demonstrate that magnetic phase transition *continues* to take place at pressures higher than 5 GPa, ruling out the possibility to consider the magnetic transition in Fe-Ni alloys in terms of only two magnetic states.<sup>10,11</sup> Moreover, Matsushita *et al.*<sup>13</sup> identified the pressure 3.5 GPa, which was viewed as HS-LS transition pressure in Refs. 10 and 11, with a clear appearance of the reentrant spin-glass-like phase, while ferromagnetic phase *began* to collapse at pressure *above* 5.5 GPa. Also, volume change between the states identified as HS and LS in Ref. 11 is less than 2%, and the bulk modulus for the LS state is too small (132 GPa) in comparison with values for nonmagnetic transition metals with the same band filling (320 GPa for Ru). All earlier calculations for Fe and Fe-Ni alloys<sup>27,28,63–69</sup> predicted that the transition between the classical Weiss HS and LS states involved much larger volume changes, around 10%. Also, bulk moduli calculated for systems with fixed spin configurations are much higher.<sup>16,27</sup> Interestingly, our present simulations with Perdew and Wang exchange correlation functional, Fig. 9(b), have some common points with the interpretation of experimental results given in Ref. 11. Indeed, our ground state is the HS ferromagnet, and the first magnetic phase transition, the spin flip transition, occurs at volumes 2.5% smaller than the equilibrium volume, while the difference in volumes between the HS FM and SF states is just below 2%. However, most likely this is a fortuitous coincidence, and in any case, the spin flip transition is identified by us as the first in the series of complex magnetic phase transitions taken place in Fe-Ni Invar upon compression rather than the final state for the HS-LS phase transition.

One common problem of several recent experimental studies<sup>9–11,84</sup> is that they do not take care of a proper experimental identification of the initial magnetic state of the alloy. Indeed, for a test of the theoretical predictions related to a possibility of the stabilization of a more complex magnetic state in  $Fe_{65}Ni_{35}$  alloy (compared to the high-spin ferromagnetic state, e.g., the spin flipped state discussed in this work or the weakly noncollinear state predicted in Ref. 16) one has to have a sample with unambiguously identified magnetic structure as a starting point, before one varies external parameters to monitor their influence on the magnetic properties of the alloy. One strategy here is to study the Invar effect for alloys with higher Ni concentration, which are definitely in the HS FM state, and to apply pressure to induce magnetic phase transitions. By monitoring deviations (or their absence!) of the experimentally obtained signals from their behavior expected for a conventional FM alloy with a fixed magnetic structure, one reduces uncertainty in the interpretation of the experimental information. Unfortunately, such a strategy requires an application of relatively high pressure, but its successful realization is possible, as was demonstrated in Ref. 8.

In contrast to the Weiss model, our present results emphasize the importance of the local chemical environment for the

magnetic transitions in Fe-Ni Invar alloys. The role of the concentration fluctuations and short-range order effects for the understanding of the Invar phenomenon was elaborated earlier by Kondorskii and Sedov<sup>89,90</sup> in their model of latent antiferromagnetism, which relates the chemical inhomogeneities to the presence of antiferromagnetic clusters inside the ferromagnetic matrix in Invar alloys. However, recent experiments show that Fe-Ni alloys in the Invar composition range show weak tendency toward ordering<sup>82</sup> rather than toward clustering, which could lead to the presence of large Fe rich precipitates. In particular, Ref. 14 points out explicitly the absence of phase separation, as well as ordered phases, in thin film Fe-Ni alloys, which still show a pronounced signature of magnetic phase transitions.

In this work we have shown that the spin flip transition induced by the local environment effects takes place in completely random alloys. Indeed, the short-range order parameters were zero for at least first four coordination shells in our supercells. Importantly, in a completely random alloy there is a nonzero probability to find Fe atoms surrounded by only Fe nearest neighbors. As a matter of fact, the probability to find 13 Fe atoms together in an fcc  $Fe_{65}Ni_{35}$  alloy is rather high, 0.37%, with an average distance between such nanoclusters about 14 Å. Moreover, a mean distance between nanoclusters composed of two shells of Fe atoms can be of the order of 35 Å. As we pointed out earlier, the Fe atoms in the Fe rich environment act as nucleation centers for the magnetic phase transition. Experiments indicate the existence of such magnetic inhomogeneities in Fe-Ni Invar alloys.<sup>12,85,91</sup>

## VII. CONCLUSIONS

In summary, we have carried out a systematic theoretical study of the magnetic structure of FeNi Invar alloys in the concentration interval of 0–50 at. % of Ni by means of two complimentary methods, the EMTO-CPA method and the PAW method as implemented in VASP. We first compared our results for pure fcc Fe calculated within three different approximations for the exchange-correlation potential and one-electron energy, the local spin density approximation, the generalized gradient approximation using the parametrization of Perdew and Wang and of Perdew, Burke, and Ernzerhof, respectively. We observed a strong influence of the exchange-correlation functional on the magnetic structure of Fe obtained as a result of the simulations. Interestingly, not only do the GGA results differ from the LSDA data, but there is also a noticeable difference between energies of different magnetic states calculated by the two different versions of the GGA. We therefore conclude that perhaps it is impossible to predict exactly the magnetic ground state of Fe and Fe-based alloys with the present day level of first-principles calculations based on the local exchange-correlation functionals. We therefore notice that while the application of novel methodologies within the electronic structure theory, like the dynamical mean-field theory, would be of high potential interest, one can still study the trends, which magnetic ground state in fcc Fe-Ni alloys show with increasing Ni concentration, and which can be reliably predicted.

Our calculations indicate that upon the variation of volume in pure fcc Fe and in fcc Fe-Ni alloys there is a transition region from the low-spin state to the high-spin ferromagnetic state. In the transition region there are many magnetic states with total energies close to each other. The region shifts off the equilibrium volume toward lower volumes with increasing Ni concentration. The ferromagnetic state is stable for most of the compositions. The partial disordered local moment state does not compete with other configurations, so earlier works which emphasize the importance of the PDLM and DLM states for Invar alloys<sup>24,26</sup> are not supported by the present study. The most important competing magnetic states are the spin spiral state and the ferrimagnetic spin flip state. The latter occurs as the first transition from the ferromagnetic high-spin state at large volumes upon decreasing of volume. Though its precise location with re-

spect to the equilibrium volume in Invar alloys depends on the approximation to the exchange-correlation functional used, we show that it is quite possible that the ground state magnetic structure of the alloys is affected by the spin flipped states. The sites with flipped spins can serve as nucleation centers for the formation of the noncollinear magnetic order in the system.

#### ACKNOWLEDGMENTS

I.A.A. would like to acknowledge useful discussions with L. Dubrovinsky. We are grateful to the Swedish Research Council and the Swedish Foundation for Strategic Research for financial support. Most of the calculations were carried out at the Swedish Infrastructure for Scientific Computing (SNIC).

- 
- <sup>1</sup>W. A. Bassett and M. S. Weathers, *J. Geophys. Res.* **95**, 21709 (1990).
- <sup>2</sup>K. Shimizu, T. Kimura, S. Furomoto, K. Takeda, K. Kontani, Y. Onuki, and K. Amaya, *Nature (London)* **412**, 316 (2001).
- <sup>3</sup>C. E. Guillaume, *C. R. Hebd. Seances Acad. Sci.* **125**, 235 (1897).
- <sup>4</sup>E. F. Wasserman, in *Ferromagnetic Materials*, edited by K. H. J. Buschow and E. P. Wohlfarth (North-Holland, Amsterdam, 1990), Vol. 5, p. 237.
- <sup>5</sup>V. Crisan, P. Entel, H. Ebert, H. Akai, D. D. Johnson, and J. B. Staunton, *Phys. Rev. B* **66**, 014416 (2002).
- <sup>6</sup>R. Lizarraga, L. Nordström, L. Bergqvist, A. Bergman, E. Sjöstedt, P. Mohn, and O. Eriksson, *Phys. Rev. Lett.* **93**, 107205 (2004).
- <sup>7</sup>A. V. Ruban, M. I. Katsnelson, W. Olovsson, S. I. Simak, and I. A. Abrikosov, *Phys. Rev. B* **71**, 054402 (2005).
- <sup>8</sup>L. Dubrovinsky, N. Dubrovinskaia, I. A. Abrikosov, M. Vennström, F. Westman, S. Carlsson, M. van Schilfhaarde, and B. Johansson, *Phys. Rev. Lett.* **86**, 4851 (2001).
- <sup>9</sup>J. P. Rueff, A. Shukla, A. Kaprolat, M. Krisch, M. Lorenzen, F. Sette, and R. Verbeni, *Phys. Rev. B* **63**, 132409 (2001).
- <sup>10</sup>F. Decremps and L. Nataf, *Phys. Rev. Lett.* **92**, 157204 (2004).
- <sup>11</sup>L. Nataf, F. Decremps, M. Gauthier, and B. Canny, *Phys. Rev. B* **74**, 184422 (2006).
- <sup>12</sup>A. R. Wildes and N. Cowlam, *J. Magn. Magn. Mater.* **272-276**, 536 (2004).
- <sup>13</sup>M. Matsushita, S. Endo, K. Miura, and F. Ono, *J. Magn. Magn. Mater.* **265**, 352 (2003).
- <sup>14</sup>E. Foy, S. Andrieu, M. Finazzi, R. Poinso, C. M. Teodorescu, F. Chevrier, and G. Krill, *Phys. Rev. B* **68**, 094414 (2003).
- <sup>15</sup>R. F. Willis and N. Janke-Gilman, *Europhys. Lett.* **69**, 411 (2005).
- <sup>16</sup>M. van Schilfhaarde, I. A. Abrikosov, and B. Johansson, *Nature (London)* **400**, 46 (1999).
- <sup>17</sup>Y. Tsunoda, *J. Phys.: Condens. Matter* **1**, 10427 (1989).
- <sup>18</sup>Y. Tsunoda, Y. Kurimoto, M. Seto, S. Kitao, and Y. Yoda, *Phys. Rev. B* **66**, 214304 (2002).
- <sup>19</sup>V. P. Antropov, M. I. Katsnelson, M. van Schilfhaarde, and B. N. Harmon, *Phys. Rev. Lett.* **75**, 729 (1995); V. P. Antropov, M. I. Katsnelson, B. N. Harmon, M. van Schilfhaarde, and D. Kusnezov, *Phys. Rev. B* **54**, 1019 (1996).
- <sup>20</sup>P. James, O. Eriksson, B. Johansson, and I. A. Abrikosov, *Phys. Rev. B* **59**, 419 (1999).
- <sup>21</sup>K. Knöpfle, L. M. Sandratskii, and J. Kübler, *Phys. Rev. B* **62**, 5564 (2000).
- <sup>22</sup>E. Sjöstedt and L. Nordström, *Phys. Rev. B* **66**, 014447 (2002).
- <sup>23</sup>S. Shallcross, A. E. Kissavos, S. Sharma, and V. Meded, *Phys. Rev. B* **73**, 104443 (2006).
- <sup>24</sup>D. D. Johnson, F. J. Pinski, J. B. Staunton, B. L. Gyorffy, and G. M. Stocks, in *Physical Metallurgy of Controlled Expansion Invar-Type Alloys*, edited by K. C. Russell and D. F. Smith (The Minerals, Metals & Materials Society, Warrendale, PA, 1990), p. 3; D. D. Johnson and W. A. Shelton, in *The Invar Effect: A Centennial Symposium*, edited by J. Wittenauer (The Minerals, Metals & Materials Society, Warrendale, PA, 1997), p. 63.
- <sup>25</sup>H. Akai, *J. Phys.: Condens. Matter* **1**, 8045 (1989).
- <sup>26</sup>H. Akai and P. H. Dederichs, *Phys. Rev. B* **47**, 8739 (1993).
- <sup>27</sup>I. A. Abrikosov, O. Eriksson, P. Söderlind, H. L. Skriver, and B. Johansson, *Phys. Rev. B* **51**, 1058 (1995).
- <sup>28</sup>M. Schröter, H. Ebert, H. Akai, P. Entel, E. Hoffmann, and G. G. Reddy, *Phys. Rev. B* **52**, 188 (1995).
- <sup>29</sup>Y. Wang, G. M. Stocks, D. M. C. Nicholson, W. A. Shelton, V. P. Antropov, and B. N. Harmon, *J. Appl. Phys.* **81**, 3873 (1997).
- <sup>30</sup>W. Olovsson and I. A. Abrikosov, *J. Appl. Phys.* **97**, 10A317 (2005).
- <sup>31</sup>I. A. Abrikosov, F. Liot, T. Marten, and E. A. Smirnova, *J. Magn. Magn. Mater.* **300**, 211 (2006).
- <sup>32</sup>Y. Wang and J. P. Perdew, *Phys. Rev. B* **44**, 13298 (1991); J. P. Perdew, J. A. Chevary, S. H. Vosko, K. A. Jackson, M. R. Pederson, D. J. Singh, and C. Fiolhais, *ibid.* **46**, 6671 (1992).
- <sup>33</sup>J. P. Perdew, K. Burke, and M. Ernzerhof, *Phys. Rev. Lett.* **77**, 3865 (1996).
- <sup>34</sup>D. M. Ceperley and B. J. Alder, *Phys. Rev. Lett.* **45**, 566 (1980).
- <sup>35</sup>J. P. Perdew and A. Zunger, *Phys. Rev. B* **23**, 5048 (1981).
- <sup>36</sup>S. H. Vosko, L. Wilk, and M. Nusair, *Can. J. Phys.* **58**, 1200 (1980).
- <sup>37</sup>L. Vitos, I. A. Abrikosov, and B. Johansson, *Phys. Rev. Lett.* **87**, 156401 (2001).

- <sup>38</sup>P. E. Blöchl, Phys. Rev. B **50**, 17953 (1994).
- <sup>39</sup>G. Kresse and J. Hafner, Phys. Rev. B **48**, 13115 (1993).
- <sup>40</sup>G. Kresse and J. Furthmüller, Comput. Mater. Sci. **6**, 15 (1996); Phys. Rev. B **54**, 11169 (1996).
- <sup>41</sup>J. S. Faulkner, Prog. Mater. Sci. **27**, 1 (1982), for a review.
- <sup>42</sup>P. Soven, Phys. Rev. **156**, 809 (1967).
- <sup>43</sup>D. W. Taylor, Phys. Rev. **156**, 1017 (1967).
- <sup>44</sup>I. A. Abrikosov and B. Johansson, Phys. Rev. B **57**, 14164 (1998).
- <sup>45</sup>A. E. Kissavos, S. I. Simak, P. Olsson, L. Vitos, and I. A. Abrikosov, Comput. Mater. Sci. **35**, 1 (2006).
- <sup>46</sup>A. Zunger, S.-H. Wei, L. G. Ferreira, and J. E. Bernard, Phys. Rev. Lett. **65**, 353 (1990).
- <sup>47</sup>L. Vitos, H. L. Skriver, B. Johansson, and J. Kollár, Comput. Mater. Sci. **18**, 24 (2000).
- <sup>48</sup>L. Vitos, Phys. Rev. B **64**, 014107 (2001).
- <sup>49</sup>L. Vitos, in *Recent Research Developments in Physics* (Transworld Research Network Publisher, Trivandrum, India, 2004), Vol. 5, pp. 103–140.
- <sup>50</sup>O. K. Andersen, O. Jepsen, and G. Krier, in *Lecture on Methods of Electronic Structure Calculations*, edited by V. Kumar, O. K. Andersen, and A. Mookerjee (World Scientific, Singapore, 1994), p. 63.
- <sup>51</sup>O. K. Andersen, C. Arcangeli, R. W. Tank, T. Saha-Dasgupta, G. Krier, O. Jepsen, and I. Dasgupta, in *Tight-Binding Approach to Computational Materials Science*, edited by P. E. A. Turchi, A. Gonis, and L. Colombo, Mater. Res. Soc. Symp. Proc. No. 491 (Materials Research Society, Pittsburgh, 1998), p. 3.
- <sup>52</sup>O. K. Andersen, T. Saha-Dasgupta, R. W. Tank, C. Arcangeli, O. Jepsen, and G. Krier, in *Electronic Structure and Physical Properties of Solids: The Uses of the LMTO Method*, edited by H. Dreysseé, Lecture Notes in Physics No. 535 (Springer-Verlag, Berlin, 2000), pp. 3–84.
- <sup>53</sup>O. K. Andersen and T. Saha-Dasgupta, Phys. Rev. B **62**, R16219 (2000).
- <sup>54</sup>L. Vitos, J. Kollár, and H. L. Skriver, Phys. Rev. B **55**, 13521 (1997).
- <sup>55</sup>J. Kollár, L. Vitos, and H. L. Skriver, in *Electronic Structure and Physical Properties of Solids: The Uses of the LMTO Method*, edited by H. Dreysé, Lecture Notes in Physics No. 535 (Springer-Verlag, Berlin, 2000), pp. 85–113.
- <sup>56</sup>H. J. Monkhorst and J. D. Pack, Phys. Rev. B **13**, 5188 (1972).
- <sup>57</sup>I. A. Abrikosov, S. I. Simak, B. Johansson, A. V. Ruban, and H. L. Skriver, Phys. Rev. B **56**, 9319 (1997).
- <sup>58</sup>J. P. Perdew and Y. Wang, Phys. Rev. B **45**, 13244 (1992).
- <sup>59</sup>J. Madsen, O. K. Andersen, U. K. Poulsen, and O. Jepsen, in *Magnetism and Magnetic Materials—1975*, edited by J. J. Becker, G. H. Lander, and J. J. Rhyne, AIP Conf. Proc. No. 29 (AIP, New York, 1976), p. 327.
- <sup>60</sup>U. K. Poulsen, J. Kollar, and O. K. Andersen, J. Phys. F: Met. Phys. **6**, L241 (1976).
- <sup>61</sup>O. K. Andersen, J. Madsen, U. K. Poulsen, O. Jepsen, and J. Kollar, Physica B & C **86-88**, 249 (1977).
- <sup>62</sup>D. M. Roy and D. G. Pettifor, J. Phys. F: Met. Phys. **7**, L183 (1977).
- <sup>63</sup>V. L. Moruzzi, P. M. Marcus, K. Schwarz, and P. Mohn, Phys. Rev. B **34**, 1784 (1986).
- <sup>64</sup>V. L. Moruzzi, Physica B **161**, 99 (1989).
- <sup>65</sup>V. L. Moruzzi, Phys. Rev. B **41**, 6939 (1990).
- <sup>66</sup>V. L. Moruzzi, Solid State Commun. **83**, 739 (1992).
- <sup>67</sup>P. Mohn, K. Schwarz, and D. Wagner, Phys. Rev. B **43**, 3318 (1991).
- <sup>68</sup>P. Entel, E. Hoffmann, P. Mohn, K. Schwarz, and V. L. Moruzzi, Phys. Rev. B **47**, 8706 (1993).
- <sup>69</sup>E. G. Moroni and T. Jarlborg, Phys. Rev. B **41**, 9600 (1990).
- <sup>70</sup>A. Georges, G. Kotliar, W. Krauth, and M. J. Rozenberg, Rev. Mod. Phys. **68**, 13 (1996).
- <sup>71</sup>G. Kotliar, S. Y. Savrasov, K. Haule, V. S. Oudovenko, O. Parcollet, and C. A. Marianetti, Rev. Mod. Phys. **78**, 865 (2006).
- <sup>72</sup>A. I. Lichtenstein, M. I. Katsnelson, and G. Kotliar, Phys. Rev. Lett. **87**, 067205 (2001).
- <sup>73</sup>L. Chioncel, L. Vitos, I. A. Abrikosov, J. Kollar, M. I. Katsnelson, and A. I. Lichtenstein, Phys. Rev. B **67**, 235106 (2003).
- <sup>74</sup>A. Grechnev, I. Di Marco, M. I. Katsnelson, A. I. Lichtenstein, J. Wills, and O. Eriksson, Phys. Rev. B **76**, 035107 (2007).
- <sup>75</sup>J. Minar, L. Chioncel, A. Perlov, H. Ebert, M. I. Katsnelson, and A. I. Lichtenstein, Phys. Rev. B **72**, 045125 (2005).
- <sup>76</sup>B. L. Györfy, A. J. Pindor, J. Staunton, G. M. Stocks, and H. Winter, J. Phys. F: Met. Phys. **15**, 1337 (1985).
- <sup>77</sup>F. Liot, S. I. Simak, and I. A. Abrikosov, J. Appl. Phys. **99**, 08P906 (2006).
- <sup>78</sup>P. Olsson, I. A. Abrikosov, L. Vitos, and J. Wallenius, J. Nucl. Mater. **321**, 84 (2003).
- <sup>79</sup>P. Olsson, I. A. Abrikosov, and J. Wallenius, Phys. Rev. B **73**, 104416 (2006).
- <sup>80</sup>A. Kissavos, Dissertation No. 1063, Linköping, LiU-Tryck, 2006.
- <sup>81</sup>A. V. Ruban, S. Khmelevskiy, P. Mohn, and B. Johansson, Phys. Rev. B **76**, 014420 (2007).
- <sup>82</sup>J. L. Robertson, G. E. Ice, C. J. Sparks, X. Jiang, P. Zschack, F. Bley, S. Lefebvre, and M. Bessiere, Phys. Rev. Lett. **82**, 2911 (1999).
- <sup>83</sup>X. Jiang, G. E. Ice, C. J. Sparks, L. Robertson, and P. Zschack, Phys. Rev. B **54**, 3211 (1996).
- <sup>84</sup>N. Cowlam and A. R. Wildes, J. Phys.: Condens. Matter **15**, 521 (2003).
- <sup>85</sup>A. Z. Menshikov and J. Schweizer, Solid State Commun. **100**, 251 (1996).
- <sup>86</sup>R. J. Weiss, Proc. R. Soc. London, Ser. A **175**, 281 (1963).
- <sup>87</sup>R. L. Mills, D. H. Liebenberg, and J. C. Bronson, J. Chem. Phys. **63**, 4026 (1975).
- <sup>88</sup>W. L. Vos and J. A. Schouten, J. Chem. Phys. **91**, 6302 (1989).
- <sup>89</sup>E. I. Kondorskii and V. L. Sedov, Zh. Eksp. Teor. Fiz. **35**, 1579 (1958) [Sov. Phys. JETP **8**, 1104 (1959)].
- <sup>90</sup>V. L. Sedov, *Antiferromagnetism of Gamma-iron. Problem of Invar* (Nauka, Moscow, 1987).
- <sup>91</sup>H. Zähres, M. Acet, W. Stamm, and E. F. Wassermann, J. Magn. Mater. **72**, 80 (1988).